Supplementary Information: Comparative analysis of Chikungunya and Zika transmission

Julien Riou[a,*], Chiara Poletto[a], and Pierre-Yves Boëlle[a]

[a]Sorbonne Universités, UPMC Univ Paris 06, INSERM, Institut Pierre Louis d'Epidémiologie et de Santé Publique (IPLESP UMRS 1136), 75012 Paris, France
[*]Corresponding author: julien.riou@iplesp.upmc.fr

Contents

1 Serial interval distribution reconstruction **1**

2 Parameter identifiability **4**

3 Model estimation **5**

4 *Free* model **9**

5 Sensitivity analysis: serial interval distribution constant in temperature **10**

6 Forward simulations **11**

7 Stan code **12**

8 References **15**

1 Serial interval distribution reconstruction

Here we provide detailed description of the reconstruction of the serial interval distribution. We used the framework we previously developed [1] for the transmission of CHIKV by *Ae. albopictus* in Réunion Island and in the West Indies [2]. It describes the different stages of disease progress in the infected humans and vectors from the development of symptoms in the primary case to development of symptoms in the secondary case. Precisely, we split the distribution of the serial interval T_{SI} in four components:

1. Time from infectiousness to symptoms in a human case T_V, distributed as:

$$T_V(t|\tau_V) = \mathcal{U}(0, \tau_V), \tag{1}$$

   where τ_V is the maximum duration from infectiousness to symptoms.

2. Time from infectiousness to infectious mosquito bite T_B, such as:

$$T_B(t|\tau_a, \tau_b) = \mathcal{U}[0, \mathcal{U}(\tau_a, \tau_b)], \tag{2}$$

   where τ_a and τ_b are the minimum and maximum durations of the infectious period, respectively.

3. Time from the bite infecting the mosquito to the bite transmitting the disease T_M, which depends on the extrinsic incubation period and is a multiple of the duration of the gonotrophic cycle of the mosquito. The mosquito bite can transmit the virus once the extrinsic incubation period in the mosquito is complete. Then, every bite, occurring at regular intervals around the average duration of one gonotrophic cycle ($\pm 1/3$), can lead to transmission. This quantity is modelled as as mixture of time to bite $T_M = \sum_i T_{M,c} 1\{C = i\}$, with $T_{M,c}$ the duration from initial mosquito infection to a bite in the c-th gonotrophic cycle, with distribution :

$$T_{M,c}(t|\gamma, \kappa) = \mathcal{U}(\kappa + (c - 1/3)\gamma, \kappa + (c + 1/3)\gamma), \tag{3}$$

where γ is the average duration of a gonotrophic cycle, κ is the duration of the extrinsic incubation period. The weights of each $T_{M,c}$ component is proportional to $e^{-\delta c \gamma}$ where δ is the mosquito mortality: this corresponds with the fraction of mosquitoes surviving long enough to bite during the c-th cycle. Depending on the gonotrophic cycle duration, the number of components in the mixture changes.

4. The incubation period (from infection to disease onset) in a secondary case T_I, which follows a lognormal distribution of mean μ_I and standard deviation σ_I.

Using these components, the serial interval is:

$$T_{SI} = -T_V + T_B + T_M + T_I \tag{4}$$

According to this formulation, the distribution of T_{SI} depends on eight parameters, five of which relate only to the human host (μ_I, σ_I, τ_V, τ_a, and τ_b), and are constant over time for a given virus (Table S1). The other three parameters (δ, γ, and κ) depend on the vector and as so are susceptible to vary according to temperature. In the following, we made the assumption that the main vector of ZIKV and CHIKV was *Ae. aegypti*. This was decided considering that *Ae. aegypti* is a competent vector of both viruses and is widely prevalent in the concerned areas [3, 4, 5, 6]. We thus searched for published estimates of the association between these three parameters and temperature in laboratory or preferably field studies involving *Ae. aegypti*. We assumed the serial interval distribution to be affected by the average temperature values during the five weeks preceding the generation of secondary cases:

1. Concerning mortality, while an association with temperature is often reported in laboratory studies, the association is not as clear in field studies: a large review and meta-analysis based on 50 experiments using mark-release-capture methods and conducted between 20.7°C and 30.1°C reported a stable estimate of the daily mortality rate of 0.29 (corresponding to a mean survival of 3.5 days) [7].

2. The duration of the gonotrophic cycle of *Ae. aegypti* has been reported between 3 and 4 days in field studies [8, 9]. A more recent laboratory study reported a quadratic association between temperature and gonotrophic cycle length [10]. Results from this study yields the following relation that was used in our subsequent analyses (Fig. S3):

$$\gamma(T) = 56.6 - 3.74 \times T - 0.064 \times T^2 \tag{5}$$

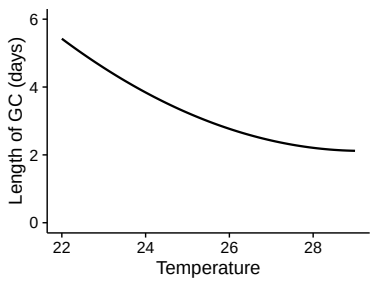

Figure S1: Association between the average duration of the gonotrophic cycle and temperature (in °C).

3. The extrinsic incubation period of CHIKV in *Ae. aegypti* mosquitoes (EIP, the time from contamination for the virus to infect the salivary glands of the vector) has been reported to be as short as 2 to 3 days (at 28°C) [11, 12]. For ZIKV, longer durations from 5-6 (at 28°C) to more than 10 days (at 24°C), have been measured in laboratory studies [13, 14]. We found no study describing the association between EIP and weather conditions for these specific combinations of vector and virus. However, studies focusing on other combinations such as DENV and *Ae. aegypti* reported a negative association with temperature [15]. As no data allowed a more precise approach, we proceeded analogously to [16, 17] by assuming that the EIP of CHIKV and ZIKV has a similar association to temperature as DENV, with disease specific calibration based on the available point estimates at 28°. This results in:

$$\kappa(T) = \kappa_{28} \times \exp(-0.21(T - 28)) \tag{6}$$

with a base value κ_{28} (i.e. measured at 28°C) fixed at 3 days for Chikungunya and at 6 days for Zika (Fig. S2).

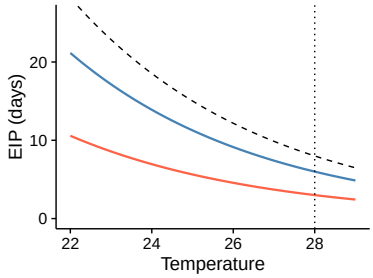

Figure S2: Association between the extrinsic incubation period and temperature for DENV (dashed black line, according to [15]), along with modelled association for CHIKV (red) and ZIKV (blue). The reference temperature of 28°C used for the model calibration is indicated by a vertical dashed line.

Stage	Symbol	Definition	CHIKV	ZIKV	Unit	References
(i)	τ_V	Maximum time from infectiousness to symptoms in humans	3	3	Days	[18, 19, 20, 21]
(ii)	$\tau_a - \tau_b$	Range of the duration of the infectious period in humans	3 - 8	4 - 7	Days	[19, 22, 21, 23]
(iii)	κ	according to past temperature $\bar{T}^\dagger$	$\kappa(\bar{T})$	$\kappa(\bar{T})$	Days	[11, 12, 14]
(iii)	γ	according to past temperature $\bar{T}^\dagger$	$\gamma(\bar{T})$	$\gamma(\bar{T})$	Days	[10]
(iii)	δ	Daily probability of death for *Ae. aegypti*	0.29	0.29	-	[7]
(iv)	μ_I, σ_I	Mean and standard deviation of the incubation period in humans	3.0, 1.3	5.9, 1.5	Days	[18, 22, 21, 24]

† *$\bar{T}$ indicates the average temperature in the five weeks preceding the generation of secondary cases.*

Table S1: Parameters used for the computation of the distribution of the serial interval.

Overall, within the range of temperature values observed during the outbreak periods in the nine territories, this resulted in a mean serial interval ranging from 1.5 to 2.7 weeks for CHIKV and from 2.2 to 4.7 weeks for ZIKV (Fig. 2 of the main paper). Reflecting the temperature charts, the changes in the serial interval were limited in Polynesia, where only the Austral islands showed variation. In the West Indies, the serial interval tended to be longer on average and more variable (Fig. S3).

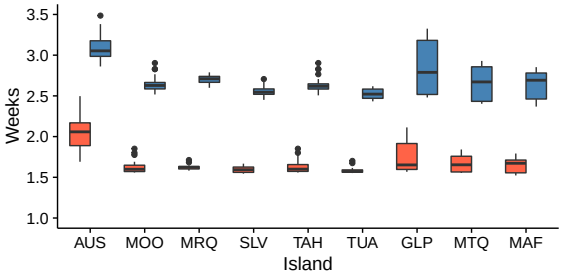

Figure S3: Distribution of the mean serial interval by island and virus over the course of the outbreaks of CHIKV (red) and ZIKV (blue).

2 Parameter identifiability

We measured the accuracy of the model in estimating the posterior distributions by testing the model with stochastic simulation of synthetic epidemics. Outbreaks of two viruses (X and Z) were simulated in five islands, with differences in transmissibility according to the island i and to the disease j. Each outbreak was initialised by 10 introductions distributed among the first five weeks. The number of secondary infections I_{ijt}, generated at each time step t by I^*_{ijt} primary cases, was drawn from a binomial distribution with S_{ijt} trials (where S_{ijt} is the number of susceptible individuals present in i at time t) and probability equal to the force of infection λ_{ijt}, the latter given by the following expression:

$$\lambda_{ijt} = \frac{\beta_{ij} I^*_{ijt}}{N_i}, \tag{7}$$

where N_i is the population of island i and β_{ij} is a transmission parameter such as:

$$\ln \beta_{ij} = b_{0i} + b_1 V_j + \epsilon_{ij}, \tag{8}$$

where b_{0i} is the island-specific factor for the transmission of virus X, b_1 a fixed parameter for the transmission of virus Z compared to virus X, V_j is 1 for virus Z and 0 for virus X, and ϵ an error term which was drawn at each time step during the simulations from a normal distribution of mean 0 and variance σ^2_ϵ. The new infections were then distributed among the following weeks according to the distribution of the serial interval. This distribution was assumed to be a gamma distribution of mean μ_{SIj} and standard deviation σ_{SIj} for each virus. The process of reporting was modelled as a binomial distribution with probability ρ_{ij}, defined as the product of an island-specific surveillance network coverage rate ψ_i and a disease-specific symptomatic rate η_j:

$$\rho_{ij} = \psi_i \times \eta_j. \tag{9}$$

Last, in order to assess whether ongoing outbreaks could lead to estimation issues, the outbreak in island *5* was truncated before its peak. One hundred stochastic runs were simulated using a fixed set of realistic values for each parameter (table S2). The *baseline* model was then fitted to the data, in order to obtain the posterior distribution of the reproductive ratio and reporting rate, which was then compared to the true values.

Parameter	Meaning	Values
b_{0i}	Island-specific intercept for virus X transmissibility	$\{0.60; 0.40; 0.50; 0.55; 0.70\}$
b_1	Transmissibility of virus Z compared to virus X	0.4
ψ_i	Island-specific probability of report of a symptomatic case	$\{0.3; 0.5; 0.6; 0.4; 0.3\}$
η_X	Probability of symptoms for virus X	0.7
η_Z	Probability of symptoms for virus Z	0.3
σ_ϵ	Standard error of the error term in transmission	0.3
N_i	Population of the five islands	$\{10000; 20000; 40000; 80000; 160000\}$
μ_{SIj}	Serial interval mean for viruses X and Z	$\{1.5; 2.5\}$
σ_{SIj}	Serial interval standard deviation for viruses X and Z	$\{0.6; 0.6\}$

Table S2: Parameters used for the simulations.

The analysis of simulated datasets showed that all parameters could be identified. Fig. S4 shows that both island-specific transmission parameter (with $R_{0i} = e^{b_{0i}}$ for disease X and $R_{0i} = e^{b_{0i}+b_1}$ for disease Z) and reporting parameter could be estimated in good agreement with the values used for simulation. Importantly, observing an epidemic only before its peak (Island *5* in the figure) did not lead to problems in estimation.

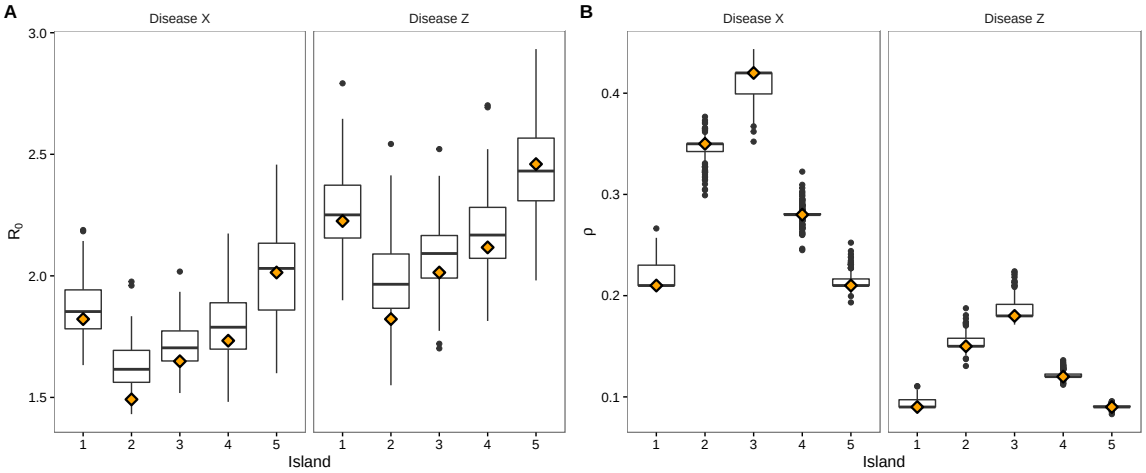

Figure S4: Identifiability of model parameters for transmission R_0 (A) and reporting ρ (B) parameters for simulated outbreaks of two hypothetical diseases (X and Z). The losange shows the parameter value chosen for the simulations, and the boxplot shows the estimated distribution of the corresponding mean of the posterior distribution of the parameter over 100 simulations. Island "5" corresponds to a partially observed epidemic (before its peak).

3 Model estimation

In this section we present the trace plots and posterior distributions of the main parameters for the *baseline* and the *weather P* model.

The *baseline* model did not include the influence of weather conditions on transmission, so that the transmission parameter was fixed for each outbreak:

$$\ln \beta_{ij} = b_i + V_j \ln \beta_D. \tag{10}$$

No issue was identified during the sampling phase, and the chains were well-mixed and converged quickly (Fig. S5 and S6). The maximum Gelman-Rubin ratio $\widehat{R}$ was estimated to 1.001.

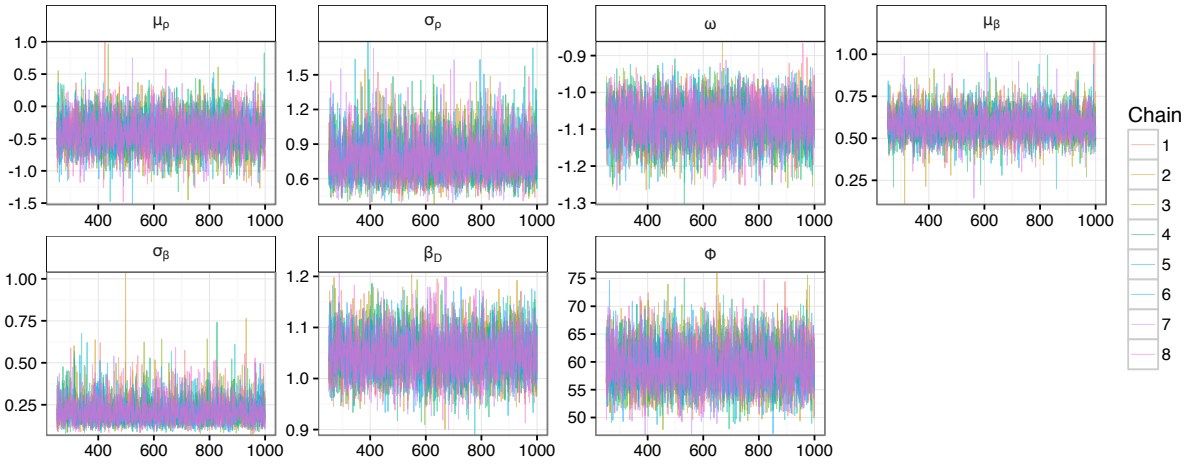

Figure S5: Trace plot of the eight chains of the *baseline* model.

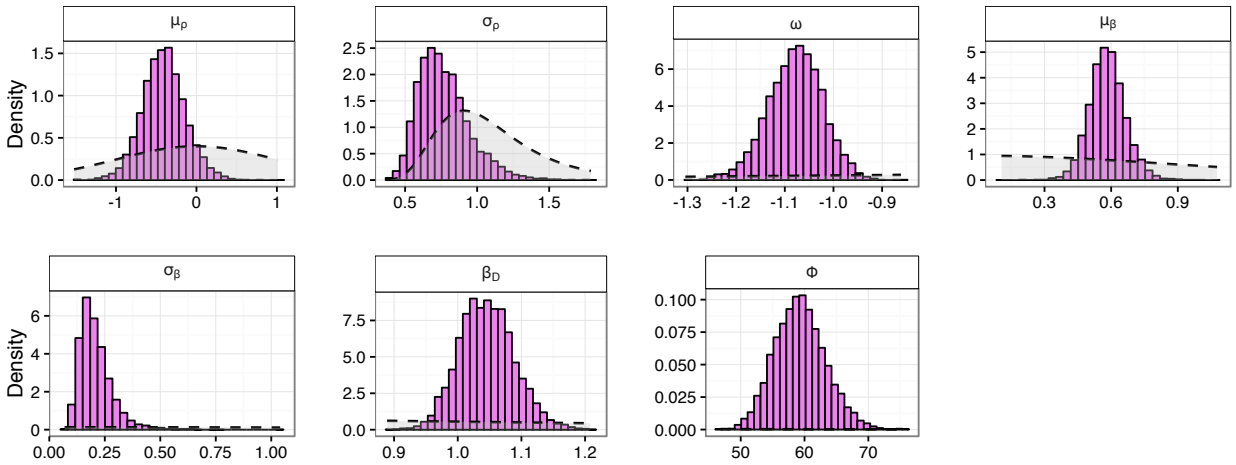

Figure S6: Posterior distributions of the parameters from the *baseline* model and corresponding prior distributions over the same range (dashed lines).

The *weather P* model included the influence of local precipitation up to eight weeks in the past, so that the transmission parameters varied with time:

$$\ln \beta_{ij} = b_i + V_j \ln \beta_D + \sum_{n=0}^{8} P_{t-l} \ln \beta_{P,l}. \tag{11}$$

The model thus accounted for the nine additional parameters $\beta_{P,l}$ (with $l = 0, \ldots, 8$) compared to the *baseline*. No issue was identified during the sampling phase, and the chains were well-mixed and converged quickly (Fig. S7 and S8). The maximum Gelman-Rubin ratio $\widehat{R}$ was estimated to 1.002. Fig. S9 shows model fit in the nine territories to allow for comparison with the baseline model's fit reported in the main paper.

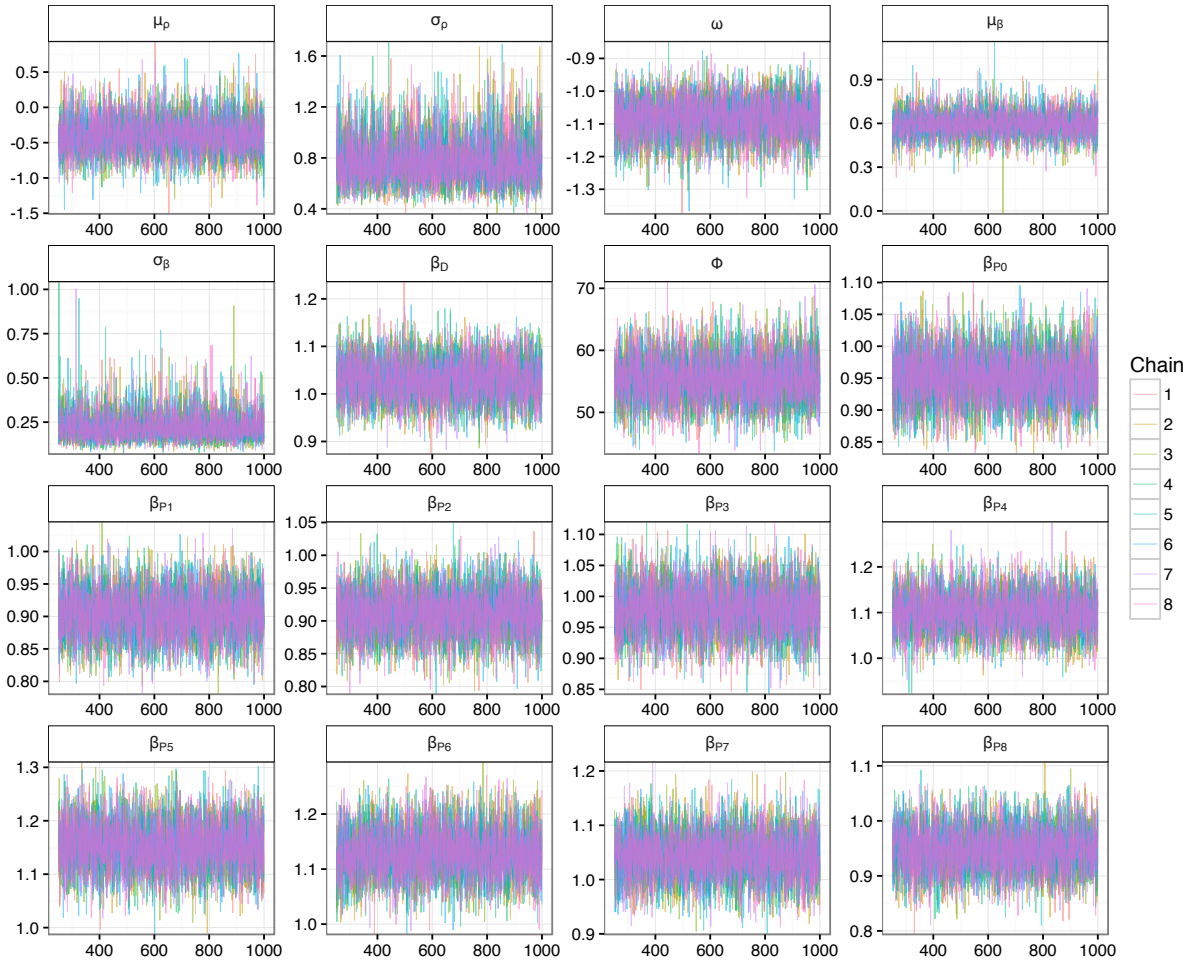

Figure S7: Trace plot of the eight chains of the *weather P* model.

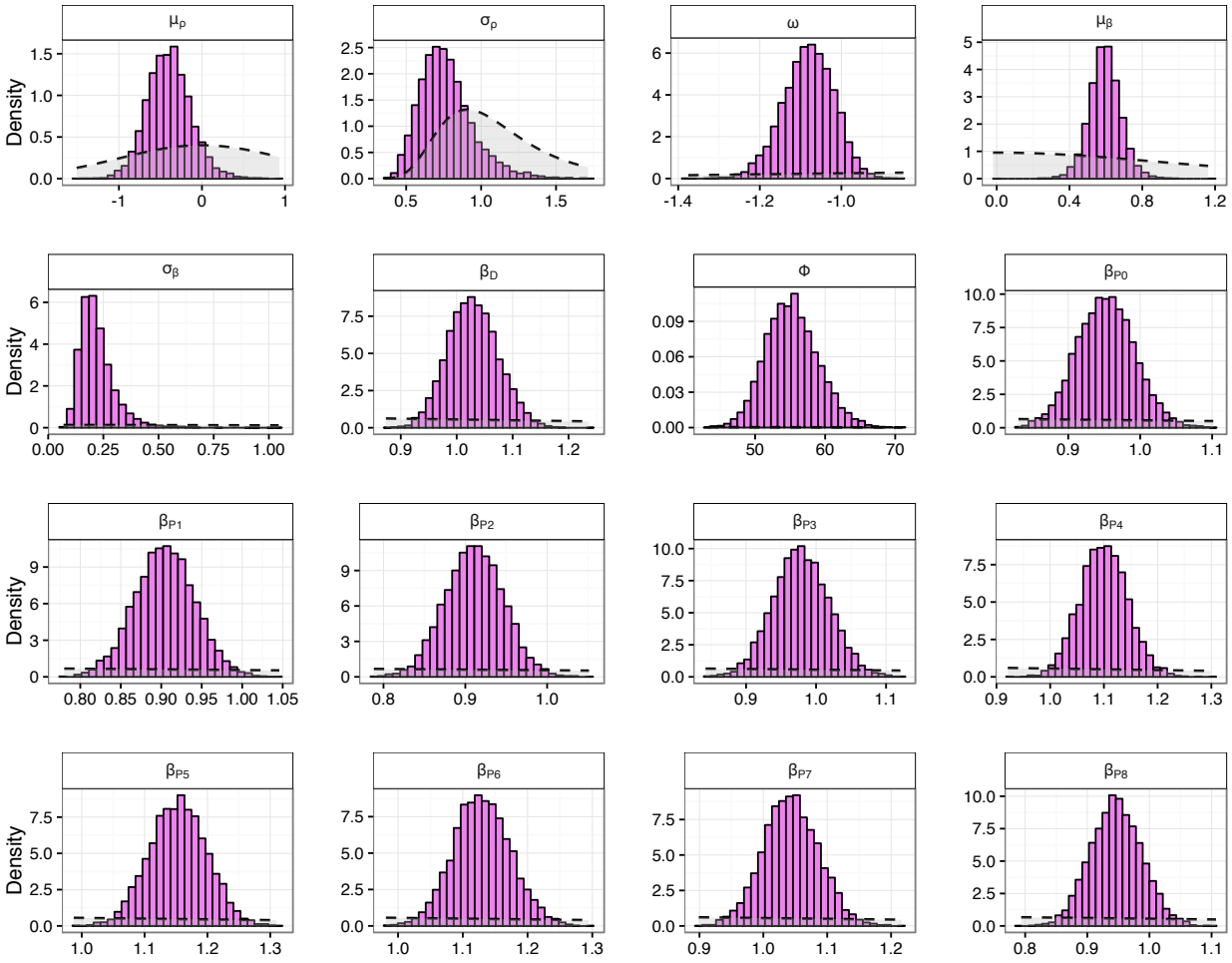

Figure S8: Posterior distributions of the parameters from the *weather P* model and corresponding prior distributions over the same range (dashed lines).

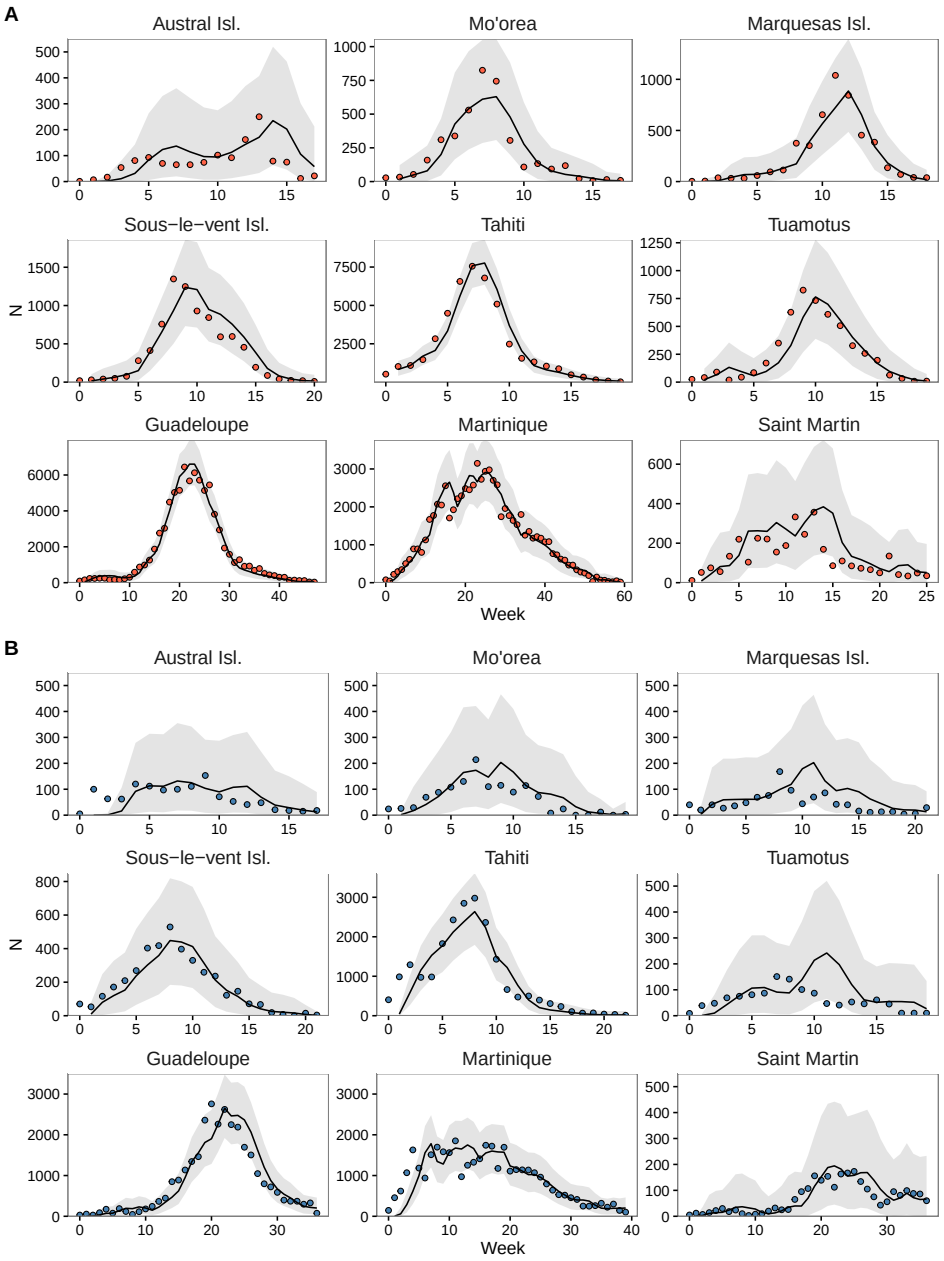

Figure S9: Observed clinical cases and *weather P* model-fitted incidence for CHIKV (A) and ZIKV (B). The grey zones correspond to 95% credible intervals.

4 *Free* model

The *baseline* model was based on the assumption of a fixed transmissibility ratio between Zika and Chikungunya when spreading in the same territory (encoded in the parameter β_D). The *free* model relaxed this assumption, the transmission parameters during two separate outbreaks of ZIKV and CHIKV occurring in the same area were estimated independently. Specifically, β consisted of two island-specific random-intercepts for CHIKV and ZIKV, respectively $b_{i,j=C}$ and $b_{i,j=Z}$:

$$\ln(\beta_{ij}) = b_{i,j=C} + b_{i,j=Z} \tag{12}$$

with:

$$b_{i,j=C} \sim \mathcal{N}(\mu_{\beta,j=C}, \sigma^2_{\beta,j=C}) \text{ and } b_{i,j=Z} \sim \mathcal{N}(\mu_{\beta,j=Z}, \sigma^2_{\beta,j=Z}). \quad (13)$$

The fit with this version of the model led to a LOOIC value equal to 5,917, with a small difference of -5 (standard error 9) compared to the *baseline*. Estimated parameters were not substantially different. The island-averaged $\bar{R}_0$ values showed no significant difference between viruses (1.78 [1.49; 2.14] for CHIKV and 1.94 [1.58; 2.41] for ZIKV), and were very close to the values estimated by the *baseline* model (1.80 [1.54; 2.12] for CHIKV and 1.88 [1.59; 2.22] for ZIKV). Reproductive numbers estimates showed higher variability in the *free* model, especially in the islands with smaller population (the Austral Isl., the Marquesas Isl., Sous-le-vent Isl., and Saint-Martin, see Fig. S10). We conclude that the comparison between the *free* and *baseline* model show no indication that CHIKV and ZIKV transmissibility have to be modelled independently.

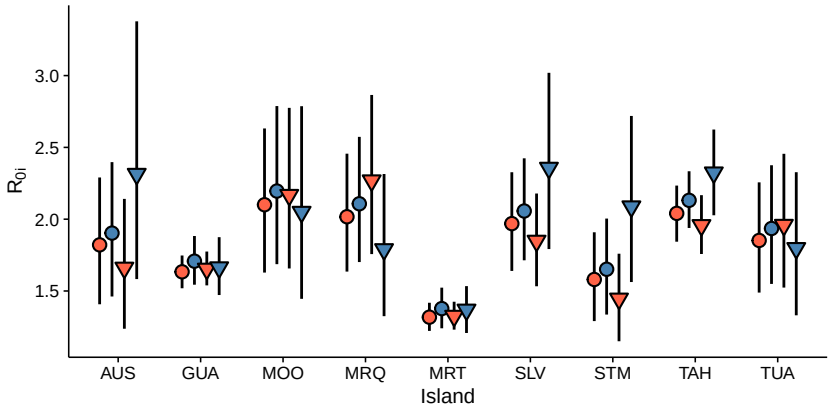

Figure S10: Island-specific basic reproduction ratio (R_{0i}) for CHIKV (red) and ZIKV (blue) for the *baseline* model (circles) and the *free* model (triangles).

5 Sensitivity analysis: serial interval distribution constant in temperature

In order to test the impact of the EIP association with temperature assumed in the model, we considered a sensitivity scenario where EIP was assumed to be a constant function of temperature. Values of EIP for each virus were taken from the observations available at 28°, namely 3 days for CHIKV and 6 days for ZIKV. Using a constant EIP led to a gamma distribution for the serial interval with $\mu_{SI} = 1.6$ weeks and $\sigma_{SI} = 0.6$ for Chikungunya, and $\mu_{SI} = 2.5$ weeks and $\sigma_{SI} = 0.7$ for Zika. The distribution resulted to be approximately constant with temperature, i.e. the temperature-dependent gonotrophic cycle alone did not introduced important temperature effects, see Fig. S11.

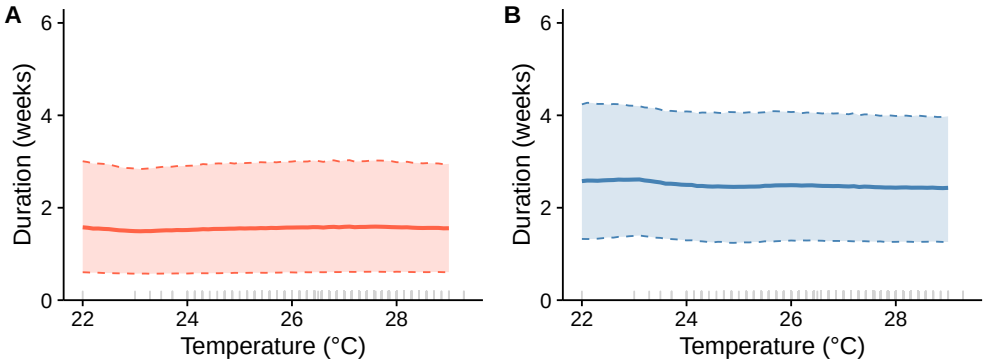

Figure S11: Mean, 2.5% and 97.5% quantiles of the serial interval duration for CHIKV (A) and ZIKV (B) according to temperature (in °C) when removing the association between the extrinsic incubation period and temperature (to be compared with Fig. 2 in the main paper).

This model version led to very similar posterior estimates for all the parameters. Considering the *baseline* model as an example we obtained island-averaged reproductive ratios equal to 1.79 [1.54; 2.10] for CHIKV and 1.87 [1.59; 2.22] for ZIKV (against 1.80 [1.54; 2.12] for CHIKV and 1.88 [1.59; 2.22] for ZIKV obtained with temperature-dependent serial interval) and island-averaged reporting rate equal to 0.40 [0.29; 0.53] and 0.19 [0.12; 0.28] for Chikungunya and Zika respectively. Similar results were also obtained for weather-related parameters, which displayed a pattern similar to the main analysis (Fig. S12). We can thus conclude that the absence of signal for the effect of temperature on transmission was not due to the inclusion of the effect of temperature in serial interval distribution.

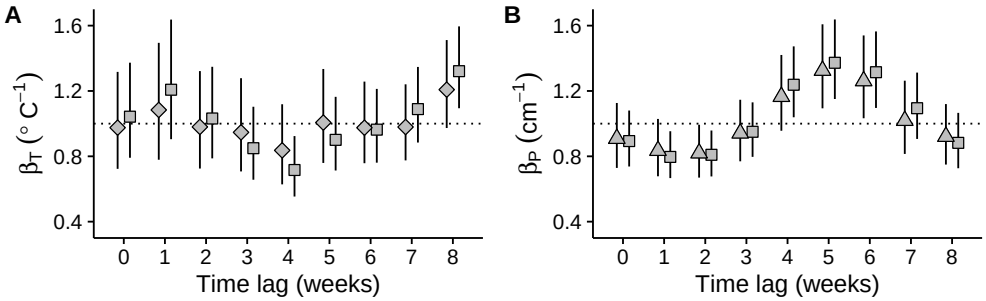

Figure S12: (A-B) Effect of a variation of 1°C of the weekly-averaged mean temperature (panel A) and of 1 cm of the weekly-averaged precipitation (panel B) on transmissiibility according to a given time lag for the three *weather* models using a fixed extrinsic incubation period (to be compared with Fig. 5).

6 Forward simulations

In Fig. 3 of the main text we presented a "one week ahead" model fit, where we compare the observed data with the conditional estimates. Our model is indeed based on a conditional description. We show here results of forward stochastic simulations of all epidemics using only the posterior distributions of the parameters and the first 5 observations in each epidemic as initial values (see Fig. S13). We computed "trajectory-wise" credible intervals for these simulations [25]. The model led to broad intervals that include the observed values in all cases.

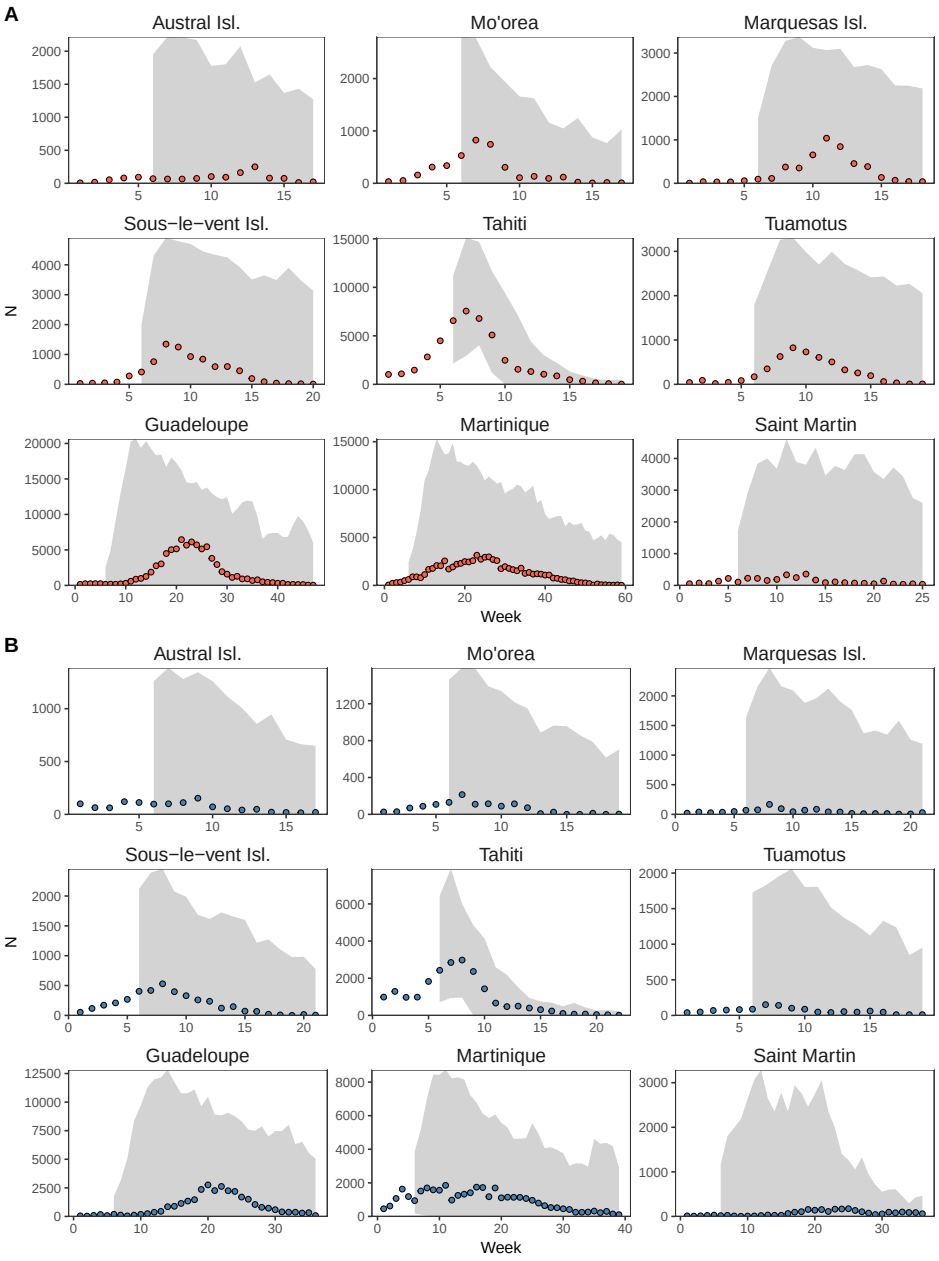

Figure S13: Observed numbers of clinical cases (circles) for CHIKV (panel A) and ZIKV (panel B), and corresponding trajectory-wise 95% credible intervals from 60,000 stochastic simulations of the epidemics using the posterior distributions of the parameters and the first five observations of each outbreak.

7 Stan code

```
data {
  int<lower=1> W; // number of records
  int<lower=1> K; // number of islands
  int<lower=1> J; // number of viruses
  int<lower=1> island[W]; // identification of island
  int<lower=0> virus[W]; // identification of virus  (0=CHIKV 1=ZIKV)
  int<lower=0> O_t[W]; // number of reported cases at time t
```

```
  real<lower=0> Ostar_t[W]; // exposure at time t
  int<lower=0> sumO_t[W]; // cumulative number of reported cases at time t
  int<lower=0> sumO_tmaxz[K]; // total number of reported ZIKV cases
  int<lower=0> sumO_tmaxc[K]; // total number of reported CHIKV cases
  int<lower=0> pop[K]; // island population
  int<lower=0> C; // number of weather covariables
  matrix[W,C] weather; // matrix of weather covariables
}

parameters {
// hyperparameters
  real mu_b0c; // distribution of b0 for CHIKV
  real<lower=0> sigma_b0c;
  real mu_rhoc; // logit of the distribution of rho for CHIKV
  real<lower=0> sigma_rhoc;

// random parameters
  real b0ic[K]; // island-specific base transmission for CHIKV
  real logitrhoc[K]; // island-specific logit reporting rate for CHIKV

// fixed parameters
  real bD; // difference of transmission for ZIKV
  real omega; // difference of reporting for ZIKV
  vector[C] bW; // effects of the weather covariables

// dispersion par
  real<lower=0,upper=100> phi;
}

transformed parameters {
  real<lower=0,upper=1> rhoc[K]; // reporting rate
  real<lower=0,upper=1> rhoz[K]; // reporting rate by island
  vector[W] theta;
  real<lower=0> beta[W];
  real<lower=0> lp[W];
  real sampledisp[W];

  for (i in 1:K) {
    rhoc[i] <- exp(logitrhoc[i]) / (1+exp(logitrhoc[i]));
    rhoz[i] <- rhoc[i]*exp(omega)/(1-rhoc[i]+rhoc[i]*exp(omega));
  }
  theta <- weather * bW;
  for( i in 1:W) {
    beta[i] <- exp( b0ic[island[i]] + bD*virus[i] + theta[i] );
    lp[i] <- beta[i] * Ostar_t[i] * ( 1 - sumO_t[i] /
     ( if_else(virus[i]==1,rhoz[island[i]],rhoc[island[i]]) * pop[island[i]]) );
    sampledisp[i] <- lp[i]/phi;
  }
}

model {
// hyperparameter priors
  mu_b0c ~ student_t(5,0,2.5);
  sigma_b0c ~ cauchy(0,2.5);
```

```
  mu_rhoc ~ normal(0,1);
  sigma_rhoc ~ inv_gamma(10,10);

// random parameter priors
  for (i in 1:K) {
    b0ic[i] ~ normal(mu_b0c,sigma_b0c);
    logitrhoc[i] ~ normal(mu_rhoc,sigma_rhoc);
  }

// fixed parameters priors
  bD ~ student_t(5,0,2.5);
  omega ~ normal(0,1);
  for (i in 1:C) {
    bW[i] ~ student_t(5,0,2.5);
  }

// likelihood
  increment_log_prob(neg_binomial_2_log(O_t,lp,sampledisp));
}
```

8 References

References

[1] P.-Y. Boëlle, G. Thomas, E. Vergu, P. Renault, A.-J. Valleron, and A. Flahault. Investigating Transmission in a Two-Wave Epidemic of Chikungunya Fever, Réunion Island. *Vector-Borne and Zoonotic Diseases*, 8(2):207–218, January 2008.

[2] S Cauchemez, M Ledrans, C Poletto, P Quenel, H De Valk, V Colizza, and PY Boëlle. Local and regional spread of chikungunya fever in the americas. *Euro surveillance: bulletin Europeen sur les maladies transmissibles= European communicable disease bulletin*, 19(28):20854, 2014.

[3] D Musso, EJ Nilles, and V-M Cao-Lormeau. Rapid spread of emerging zika virus in the pacific area. *Clinical Microbiology and Infection*, 20(10):O595–O596, 2014.

[4] Tu-Xuan Nhan, Aurore Claverie, Claudine Roche, Anita Teissier, Marc Colleuil, Jean-Marie Baudet, Van-Mai Cao-Lormeau, and Didier Musso. Chikungunya virus imported into french polynesia, 2014. *Emerg Infect Dis*, 20(10):1773–4, 2014.

[5] Vaea Richard, Tuterarii Paoaafaite, and Van-Mai Cao-Lormeau. Vector competence of aedes aegypti and aedes polynesiensis populations from french polynesia for chikungunya virus. *PLOS Negl Trop Dis*, 10(5):e0004694, 2016.

[6] Isabelle Leparc-Goffart, Antoine Nougairede, Sylvie Cassadou, Christine Prat, and Xavier De Lamballerie. Chikungunya in the americas. *The Lancet*, 383(9916):514, 2014.

[7] Oliver J Brady, Michael A Johansson, Carlos A Guerra, Samir Bhatt, Nick Golding, David M Pigott, Hélène Delatte, Marta G Grech, Paul T Leisnham, Rafael Maciel-de Freitas, et al. Modelling adult aedes aegypti and aedes albopictus survival at different temperatures in laboratory and field settings. *Parasites & vectors*, 6(1):1–12, 2013.

[8] GAH McClelland, GR Conway, et al. Frequency of blood feeding in the mosquito aedes aegypti. *Nature*, 23:485–6, 1971.

[9] PM Sheppard, WW Macdonald, RJ Tonn, and B Grab. The dynamics of an adult population of aedes aegypti in relation to dengue haemorrhagic fever in bangkok. *The journal of animal ecology*, pages 661–702, 1969.

[10] Lauren B Carrington, M Veronica Armijos, Louis Lambrechts, Christopher M Barker, and Thomas W Scott. Effects of fluctuating daily temperatures at critical thermal extremes on aedes aegypti life-history traits. *PLoS One*, 8(3):e58824, 2013.

[11] Mathieu Dubrulle, Laurence Mousson, Sara Moutailler, Marie Vazeille, and Anna-Bella Failloux. Chikungunya virus and aedes mosquitoes: saliva is infectious as soon as two days after oral infection. *PloS one*, 4(6):e5895, 2009.

[12] Myrielle Dupont-Rouzeyrol, Valérie Caro, Laurent Guillaumot, Marie Vazeille, Eric D'Ortenzio, Jean-Michel Thiberge, Noémie Baroux, Ann-Claire Gourinat, Marc Grandadam, and Anna-Bella Failloux. Chikungunya virus and the mosquito vector aedes aegypti in new caledonia (south pacific region). *Vector-Borne and Zoonotic Diseases*, 12(12):1036–1041, 2012.

[13] JPT Boorman and JS Porterfield. A simple technique for infection of mosquitoes with viruses transmission of zika virus. *Transactions of the Royal Society of Tropical Medicine and Hygiene*, 50(3):238–242, 1956.

[14] MeiZhi Irene Li, Pei Sze Jeslyn Wong, Lee Ching Ng, and Cheong Huat Tan. Oral susceptibility of singapore aedes (stegomyia) aegypti (linnaeus) to zika virus. *PLoS Negl Trop Dis*, 6(8):e1792, 2012.

[15] Miranda Chan and Michael A Johansson. The incubation periods of dengue viruses. *PloS one*, 7(11):e50972, 2012.

[16] Michael A Johansson, Ann M Powers, Nicki Pesik, Nicole J Cohen, and J Erin Staples. Nowcasting the spread of chikungunya virus in the americas. *PloS one*, 9(8):e104915, 2014.

[17] T. Alex Perkins, Amir S. Siraj, Corrine W. Ruktanonchai, Moritz U. G. Kraemer, and Andrew J. Tatem. Model-based projections of Zika virus infections in childbearing women in the Americas. *Nature Microbiology*, 1:16126, July 2016.

[18] Clarence J. Peters and Joel M. Dalrymple. Alphaviruses. In *Virology*, page an. Fields, B, Knipe, D, New York, raven press edition, 1990.

[19] Hatsadee Appassakij, Paiwon Khuntikij, Marisa Kemapunmanus, Rochana Wutthanarungsan, and Khachornsakdi Silpapojakul. Viremic profiles in asymptomatic and symptomatic chikungunya fever: a blood transfusion threat? *Transfusion*, 53(10pt2):2567–2574, 2013.

[20] Olivier Schwartz and Matthew L. Albert. Biology and pathogenesis of chikungunya virus. *Nat Rev Micro*, 8(7):491–500, July 2010.

[21] RN Charrel, I Leparc-Goffart, S Pas, X de Lamballerie, M Koopmans, and C Reusken. State of knowledge on zika virus for an adequate laboratory. *Bulletin of the World Health Organization*, 2016.

[22] J Erin Staples, Robert F Breiman, and Ann M Powers. Chikungunya fever: an epidemiological review of a re-emerging infectious disease. *Clinical Infectious Diseases*, 49(6):942–948, 2009.

[23] Musso D Mallet HP, Vial AL. Bilan de l'épidémie a virus zika en polynésie francaise 2013–2014. *Bulletin d'Information Sanitaires, Epidemiologiques et Statistiques*, 2015.

[24] Justin T Lessler, Cassandara T Ott, Andrea C Carcelen, Jacob M Konikoff, Joe Williamson, Qifang Bi, Lauren M Kucirka, Derek AT Cummings, Nicholas G Reichd, and Lelia H Chaissona. Times to key events in the course of zika infection and their implications: a systematic review and pooled analysis. *Bull World Health Organ [Internet]*, 2016.

[25] Laura Temime and Guy Thomas. Estimation of balanced simultaneous confidence sets for sir models. *Communications in Statistics—Simulation and Computation®*, 35(3):803–812, 2006.